STEM CELLS®

REGENERATIVE MEDICINE

Ex Vivo Molecular Rejuvenation Improves the Therapeutic Activity of Senescent Human Cardiac Stem Cells in a Mouse Model of Myocardial Infarction

ELISA AVOLIO,[a] GIUSEPPE GIANFRANCESCHI,[a] DANIELA CESSELLI,[a] ANGELA CARAGNANO,[a] EMMANOUIL ATHANASAKIS,[a] RAJESH KATARE,[b] MARCO MELONI,[c] ANITA PALMA,[a] ARIANNA BARCHIESI,[a] CARLO VASCOTTO,[a] BARBARA TOFFOLETTO,[a] ELISA MAZZEGA,[a] NICOLETTA FINATO,[a] GIUSEPPE ARESU,[d] UGOLINO LIVI,[d] COSTANZA EMANUELI,[c] GIACINTO SCOLES,[a] CARLO ALBERTO BELTRAMI,[a] PAOLO MADEDDU,[b] ANTONIO PAOLO BELTRAMI[a]

Key Words. Stem cells • Myocardial infarction • Cellular senescence • Heart failure

[a]Department of Medical and Biological Sciences and [d]Department of Experimental Medical and Clinical Sciences, University of Udine, Udine, Italy; [b]Experimental Cardiovascular Medicine and [c]Vascular Pathology and Regeneration, Bristol Heart Institute, School of Clinical Sciences, University of Bristol, Bristol, United Kingdom

Correspondence: Antonio Paolo Beltrami, Ph.D., M.D., Istituto di Anatomia Patologica, Università degli Studi di Udine, C.S.L., Azienda Ospedaliero Universitaria di Udine, 33100 Udine, Italy. Telephone: 390432559477; Fax: 390432559420; e-mail: antonio.beltrami@uniud.it

Received December 12, 2013; accepted for publication April 17, 2014; first published online in STEM CELLS *EXPRESS* May 6, 2014.

1066-5099/2014/$30.00/0

http://dx.doi.org/10.1002/stem.1728

ABSTRACT

Cardiac stem cells (CSC) from explanted decompensated hearts (E-CSC) are, with respect to those obtained from healthy donors (D-CSC), senescent and functionally impaired. We aimed to identify alterations in signaling pathways that are associated with CSC senescence. Additionally, we investigated if pharmacological modulation of altered pathways can reduce CSC senescence in vitro and enhance their reparative ability in vivo. Measurement of secreted factors showed that E-CSC release larger amounts of proinflammatory cytokine IL1β compared with D-CSC. Using blocking antibodies, we verified that IL1β hampers the paracrine protective action of E-CSC on cardiomyocyte viability. IL1β acts intracranially inducing IKKβ signaling, a mechanism that via nuclear factor-κB upregulates the expression of IL1β itself. Moreover, E-CSC show reduced levels of AMP protein kinase (AMPK) activating phosphorylation. This latter event, together with enhanced IKKβ signaling, increases TORC1 activity, thereby impairing the autophagic flux and inhibiting the phosphorylation of Akt and cAMP response element-binding protein. The combined use of rapamycin and resveratrol enhanced AMPK, thereby restoring downstream signaling and reducing IL1β secretion. These molecular corrections reduced E-CSC senescence, re-establishing their protective activity on cardiomyocytes. Moreover ex vivo treatment with rapamycin and resveratrol improved E-CSC capacity to induce cardiac repair upon injection in the mouse infarcted heart, leading to reduced cardiomyocyte senescence and apoptosis and increased abundance of endogenous c-Kit$^+$ CSC in the peri-infarct area. Molecular rejuvenation of patient-derived CSC by short pharmacologic conditioning boosts their in vivo reparative abilities. This approach might prove useful for refinement of CSC-based therapies. STEM CELLS *2014;32:2373–2385*

INTRODUCTION

Cellular senescence, a specialized form of permanent growth arrest caused by stressful stimuli, is a more dynamic process than we previously thought [1, 2]. Stem cells senesce too; their ageing is accelerated by cardiovascular risk factors and contributes to disruption of tissue homeostasis and repair [3, 4]. This is also true for stem cells harbored within the human heart. Cardiac stem cells (CSC) isolated from failing explanted hearts (E-CSC) display, with respect to those isolated from healthy donor hearts (D-CSC), a significant accumulation of senescent cells in vitro [5]. However, the impact that cellular senescence exerts on CSC's in vivo reparative abilities is still undetermined. This issue is particularly relevant, given the encouraging results of autologous CSC-based clinical trials, which showed preliminary evidence of therapeutic efficacy [6, 7]. We have previously documented that the availability of endogenous CSC is increased by stabilization of prosurvival signaling with Pim-1 genetic engineering [8] or by controlling redox state with an activator of the pentose phosphate pathway [9]. However, to the best of our knowledge, no previous study has targeted key molecular networks implicated in stem cell dysfunction.

To gain insights into ageing mechanisms, we first investigated if the secretome of E-CSC is enriched in soluble factors able both to strengthen senescence in an autocrine fashion and to induce it paracrinally on neighboring cardiac cells (i.e., senescence-associated secretory phenotype—SASP) [10]. We specifically focused on IL1β, given the role of this interleukin in inflammation. The secretion of IL1β is highly

regulated both transcriptionally and post-transcriptionally. Nuclear factor (NF)-κB binds to the IL1β promoter stimulating the expression of the 35-kDa pro-IL1β, which is inactive and remains within the cell [11]. To be secreted, IL1β needs to be processed by the inflammasome, a molecular platform able to activate caspase 1 (previously known as interleukin-1 converting enzyme) [11]. Since impaired AMP protein kinase (AMPK) activation and autophagy are involved in the activation of the inflammasome and IL1β secretion in myeloid cells [12], we compared the activation status of this pathway in D- and E-CSC. Next, we studied the molecular networks interconnected with AMPK signaling that have been involved in cell senescence [13]. Among the most prominent ones, we focused on the mTOR-signaling pathway. Intriguingly, this latter is inhibited by AMPK [13] but may be activated by IKKβ in response to IL1β stimulation [14, 15]. mTOR plays a central role in cell senescence since its inactivation converts cellular senescence (a permanent exit from the cell cycle) into quiescence (a reversible cell cycle withdrawal) [16], while its activation may determine stem cell exhaustion and aging [17]. mTOR is required for the activity of two multiprotein complexes (i.e., TORC1 and TORC2) [18]. TORC1 is rapamycin sensitive, regulates both ribosomal biogenesis (phosphorylating the 4E-binding proteins, 4E-BPs), and protein synthesis (phosphorylating the ribosomal S6 kinase, S6K), and inhibits autophagy [19]. TORC2 is rapamycin insensitive and activates Akt via phosphorylation at Ser^{473}. Importantly, TORC1 antagonizes TORC2, inhibiting the PI3K-Akt pathway [18]. Finally, we analyzed cAMP response element-binding protein (CREB), a transcription factor that can be phosphorylated by AMPK [20] and is involved in age-related diseases [21, 22] and in the regulation of several organism activities, ranging from metabolism—via Sirt1—[23] to the circadian rhythm-regulating miRNA-132 [24].

To identify a pharmacological treatment able to reverse the above-described molecular alterations and, eventually, E-CSC senescence in vitro, we tested rapamycin and resveratrol. The first drug was used for its reported ability to inhibit TORC1, thus converting cellular senescence into quiescence [25]. Resveratrol was chosen both for its well-established positive effects on the cardiovascular system [26] and for its ability to suppress cell senescence, possibly reducing, either directly or indirectly, TORC1 activation [27–30].

In conclusion, we identified a drug treatment that, combining rapamycin and resveratrol, activates AMPK, reduces IL1β secretion, and is able to attenuate E-CSC senescence in vitro. Additionally, we demonstrated that E-CSC are characterized by a reduced ability to repair myocardial infarction (MI) in vivo. Importantly, we newly show that a combined ex vivo drug-treatment with rapamycin and resveratrol restores the reparative ability of senescent CSC to control levels.

Materials and Methods

Detailed Supporting Information methods are available online.

Human CSC Isolation and Culture

Atrial samples were collected both from donor hearts ($n = 14$) and from explanted hearts ($n = 20$) of patients undergoing cardiac transplantation at the University Hospital of Udine (Supporting Information Table S1). The study was approved by the Ethics Committee of Udine (reference number 47831) and written consent was obtained from each patient.

Atrial fragments were first disaggregated mechanically with scalpels and then enzymatically dissociated, in a 0.25% Collagenase type II solution (Worthington, Lakewood, NJ, http://www.worthington-biochem.com) for 15–20 minutes at 37°C. The cell suspension was first centrifuged at 100*g* for 1 minute to remove myocytes and subsequently at 500*g* for 10 minutes and filtered through a sieve whose pore size is 40 μm (BD Biosciences, Italy, http://www.bdbiosciences.com/). Isolated cells (1.5×10^6) were then plated in 100-mm dishes and cultured as in [31].

Mouse Model of MI

Eight-week-old female SCID/beige mice were used for in vivo experiments. MI was induced by occlusion of the left anterior descending coronary artery, followed by injection of CSC (3×10^5 cells per heart) or vehicle at three different sites along the infarct border zone, as in [32]. Two weeks later, MI animals were sacrificed, hearts were arrested in diastole with $CdCl_2$, and perfusion-fixed with 10% (vol/vol) formalin. Dimensional and functional parameters were measured with a high-frequency, high-resolution echocardiography system (Vevo 770, VisualSonics, Toronto, Canada, http://www.visualsonics.com) both before coronary artery ligation (Supporting Information Fig. S1), and 2 weeks post-MI. Left ventricular pressure was measured with a 1.4F Millar catheter (Millar Instruments, Houston, TX, http://millar.com) before animals were euthanized.

Histological Studies

Formalin-fixed, paraffin-embedded 4 μm sections were used. Scar size was evaluated on Azan-Mallory stained sections. See Supporting Information Table S2 and Expanded Methods.

Western Blot and ELISA Analyses

Total lysates and cell culture supernatants from D-CSC, untreated- and drug-treated-E-CSC were used for Western blotting and ELISA, respectively. See Supporting Information Table S2 and Expanded Methods.

Ischemia/Reperfusion Injury in Isolated Cardiomyocytes

Cardiomyocytes isolated from four adult male Wistar rat hearts were subjected to simulated ischemia (SI) for 40 minutes followed by 17 hours of ReOxygenation (RO) in myocyte culture medium conditioned or not by CSC. See Expanded Methods.

Statistical Analyses

Characteristics of the study population are described using means ± SEM. Data were analyzed for normal distribution by Kolmogorov-Smirnov test. *T*-test or Mann-Whitney *U* test, as appropriate, was used to compare continuous variables between two groups. Drug-treatment assays were analyzed by repeated measurements one-way Anova followed by Bonferroni post-test or by Kruskal-Wallis followed by Dunn's post-test, as appropriate. In order to distinguish the effects of age and pathology on CSC senescence parameters (dependent variables), a univariate general linear model was used in which pathology was considered as fixed factor and age as covariate. Probability values (p) less than .05 were considered significant. Results are shown as means ± SEM. Analyses were conducted with Prism, version 4.0c (Graphpad Software, La Jolla, CA, http://www.graphpad.com) and SPSS20 (IBM, Armonk, NY, http://www.ibm.com/) for Macintosh software.

Results

CSC Isolated from Failing Hearts Are Senescent

CSC, dissociated from atrial fragments of both normal and pathologic human hearts, can be expanded in vitro as proliferating cultures of undifferentiated c-Kit-positive cells (Fig. 1A), cloned, and differentiated toward myocyte (Fig. 1B), smooth muscle (Fig. 1C), and endothelial (Fig. 1D) lineages [5, 31].

Undifferentiated D- and E-CSC share a similar surface immunophenotype, with the only exception of CD49a which was more expressed by E-CSC (Fig. 1E, Supporting Information Fig. S2) [5]. As expected, cultures of undifferentiated E-CSC are significantly enriched in cells displaying typical senescence features, such as the expression of the cyclin-dependent kinase inhibitor $p16^{INK4a}$ (Fig. 1F–1H) or the persistence of an activated DNA damage response—DDR (Fig. 1l–1K) [1]. Furthermore, E-CSC are less proliferating (Fig. 1L–1N, Supporting Information Fig. S3) and more apoptotic (Fig. 1O–1Q) as compared to D-CSC. Although both age and pathology may play a role in the senescence process [5], univariate linear model analysis showed that the pathological status is, in this case study, the only independent predictor for $p16^{INK4a}$ ($p < .0001$), DDR ($p = .004$), Ki67 ($p < .0001$), and TUNEL ($p = .02$) levels in CSC.

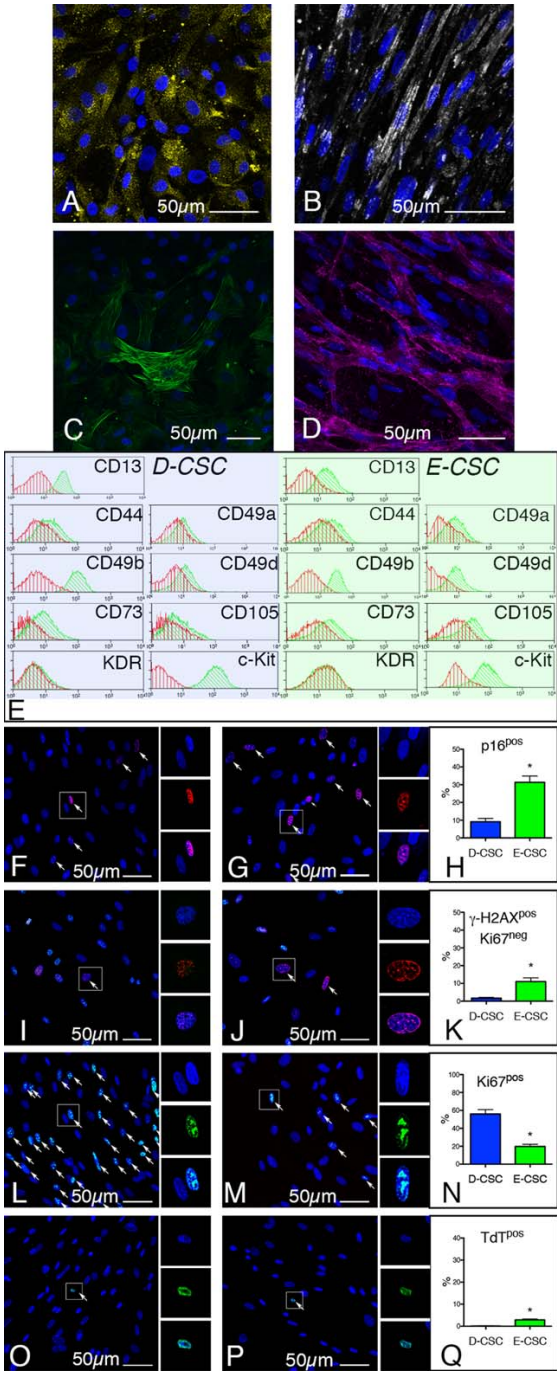

E-CSC Release an IL1b-Rich Secretome that Fails to Protect Cardiomyocytes from Ischemia Reperfusion Injury

In order to determine whether a SASP characterizes E-CSC, we measured, in their culture supernatants, 14 senescence-associated cytokines and growth factors. Both D- and E-CSC secrete similar levels of basic fibroblast growth factor (bFGF), hepatocyte growth factor (HGF), vascular endothelial growth factor (VEGF), IL6, and IL8. However, IL1β was more abundant in E-CSC culture supernatants (Fig. 2A). Next, we evaluated the biological effect of the CSC secretome on the apoptosis and senescence of adult rat cardiomyocytes exposed in vitro to SI/RO, according to the protocol illustrated in Figure 2B. Postconditioning cardiomyocytes with the D-CSC culture supernatant significantly reduced both these processes, as assessed by measurements of caspase 3/7 activity (Fig. 2C) and frequency of p16-positive cells (Fig. 2D, 2E). In contrast, the conditioned medium of E-CSC did not exert any protective effect. The addition of an anti-IL1β antibody did not modify the antisenescence and antiapoptotic action of D-CSC medium (Supporting Information Fig. S4), but restored these properties

Figure 1. CSC Characterization. Undifferentiated CSC express cKit (**A**, yellow) and can differentiate into cardiac myosin positive (**B**, white), smooth muscle positive (**C**, green), and CD31 positive (**D**, purple) cells. Representative flow-cytometry histograms of cultured D- and E-CSC **(E)** analyzed after three passages in vitro. Isotype control IgG-staining profiles (red histogram) are shown superimposed to specific antibody staining profiles (green histogram). Confocal images of cultured D-CSC **(F, I, L, O)** and E-CSC **(G, J, M, P)** illustrating: the nuclear expression of the senescence marker $p16^{INK4A}$ (arrows, red) both in D-CSC (F) and E-CSC (G); the presence of cells showing a persistent DDR (i.e., expressing the γH2AX histone variant—arrows, red, in the absence of Ki67—green) both in D-CSC (I) and E-CSC **(J)**; the presence of D-CSC (L) and E-CSC (M) cycling cells (Ki67, arrows, green); the presence of apoptotic D-CSC (O) and E-CSC (P) (TUNEL, arrows, green). Nuclei are shown by the blue fluorescence of 4′,6-diamidino-2-phenylindole. Split channel images of the cells comprised in the squares are shown at a higher magnification in the right portion of each figure. Histograms **(H, K, N, Q)** represent the fraction of cells (%) positive to the above-described immuno-stainings. *, $p < .05$ versus D-CSC. Abbreviations: D-CSC, cardiac stem cells isolated from donor hearts; E-CSC, cardiac stem cells isolated from explanted, failing hearts.

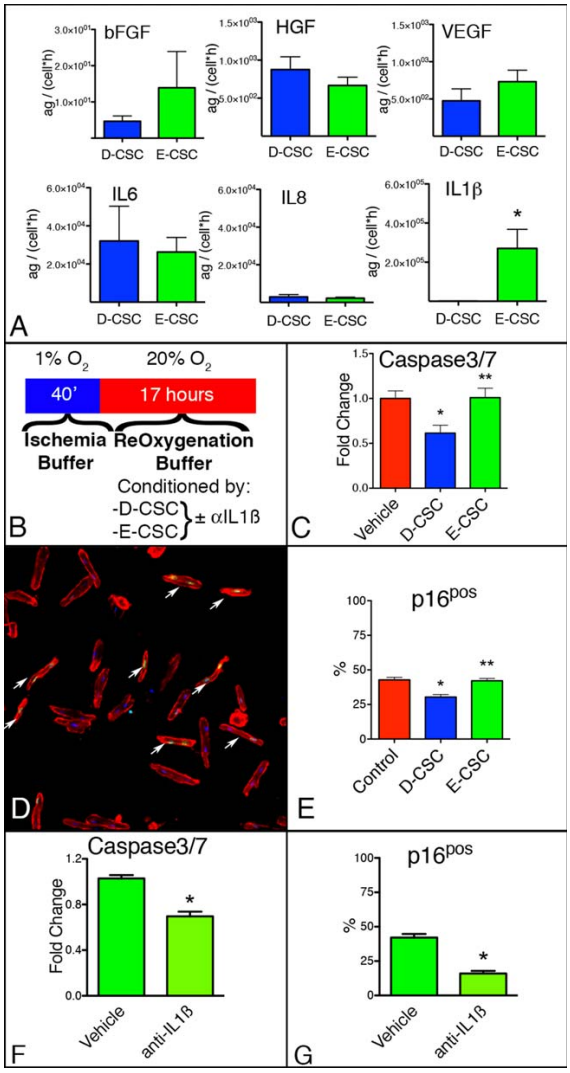

Figure 2. E-CSC release the detrimental cytokine IL1β. Histograms representing the quantity of proangiogenic growth factors (VEGF, HGF, and bFGF) and inflammatory (IL6, IL8, and IL1β) cytokines released by D-CSC and E-CSC in the culture supernatant **(A)**. Quantities of secreted factors were normalized for the volume of the collected supernatant, CSC number, and hours of incubation. **(B–G)** Effects of CSC culture supernatant on isolated adult rat cardiomyocytes exposed to a SI/RO protocol (B). Caspase activity was dosed by a luminescent assay and normalized with the activity of myocytes exposed to vehicle (C), while $p16^{pos}$ (arrows, green, D) cardiomyocytes were identified by immunofluorescence. Myocyte cytoplasm and nuclei were labeled by alpha-sarcomeric actin antibody (red) and 4′,6-diamidino-2-phenylindole (blue), respectively. Histograms (C, E, F, G) summarize quantitative data of the effect exerted by the culture supernatant of: D- versus E-CSC (C, E) or E-CSC added or not with anti-IL1β antibody (F, G) on myocyte apoptosis and senescence. *, **, $p < .05$ versus I, and II bar, respectively. Abbreviations: bFGF, basic fibroblast growth factor; HGF, hepatocyte growth factor; VEGF, vascular endothelial growth factor; D-CSC, cardiac stem cells isolated from donor hearts; E-CSC, cardiac stem cells isolated from explanted, failing hearts.

when added to the E-CSC medium prior to incubation with cardiomyocytes (Fig. 2F, 2G). Altogether these results indicate that the secretion of IL1β by E-CSC abrogates the protective effect of CSC secretome on cardiomyocyte apoptosis and senescence.

Molecular Pathways Associated with E-CSC Senescence and Secretory Phenotype: (NF)-ĵB, AMPK, mTOR, and Autophagy

Next, we evaluated the transcriptional and post-transcriptional regulation of IL1β release. The engagement of IL1β with its receptor (IL1R) may induce IL1β transcription, by activating the canonical NF-κB signaling pathway, which involves mostly IKKβ- and NEMO-dependent degradation of IκBs [15, 33] (Fig. 3A). Consistently, we observed that the levels of IKKβ phosphorylated on Ser^{177} were significantly higher in patient-derived E-CSC (Fig. 3B), and the addition of an anti-IL1β antibody to E-CSC culture medium reduced IKKβ phosphorylation (Fig. 3C). Additionally, E-CSC expressed significantly higher levels of both pro-IL1β and microRNA-146a, another validated NF-κB transcriptional target that may be induced by the same IL1β [34, 35] (Fig. 3D).

The post-translational level of regulation involves the activation of the inflammasome. In line, E-CSC were enriched in cleaved Caspase 1 (Fig. 3E), while the addition of an inhibitor of Caspase 1 activity to E-CSC reduced the release of IL1β (Fig. 3F). E-CSC showed also a significant reduction in the levels of activated AMPK (Fig. 4A). This was coupled with an enhanced activity of TORC1, as suggested by three lines of evidence: first, S6K, one TORC1 downstream target, tended to be more phosphorylated in E-CSC (Fig. 4B); second, Akt, which is negatively regulated by TORC1 [18], showed decreased Ser^{473} phosphorylation in E-CSC (Fig. 4C); third, autophagy, which is repressed by TORC1 [19], is consistently altered in E-CSC. In support of the last assumption, although enriched in Atg3, Atg7, and LC3BII, E-CSC showed significantly increased levels of p62, a ubiquitin-binding scaffold protein also called sequestosome 1 (SQSTM1), whose accumulation is suggestive of a block in the autophagic degradation (Fig. 4D). Altogether these results indicate that the increased release of IL1β derives from the concomitant increase in NF-κB-driven pro-IL1β gene transcription and inflammasome activation. This latter event is likely to be related to reduced AMPK activation, increased TORC1 activity, associated with an arrest in the autophagic flux.

Besides their effects on autophagy and inflammasome activation, both AMPK and Akt can phosphorylate CREB on Ser^{133}, thereby activating downstream effectors [36]. Consistently, phospho-$CREB^{Ser133}$ was higher in D-CSC as compared to E-CSC (Fig. 4E). While Sirt1, a downstream target of CREB signaling [23], did not differ between the two cell types, microRNA-132 (Fig. 4F, 4G), a transcriptional target of CREB, was significantly more abundant in D-CSC, supporting a secondary involvement of CREB signaling in E-CSC senescence.

Rapamycin and Resveratrol Cooperatively Reduce E-CSC Senescence

Subsequently, we tried both to revert E-CSC senescence and to restore the in vitro protective effects of CSC by a short ex vivo pharmacological treatment. To this aim, first we performed a pilot titration study, testing the acute effect of 1

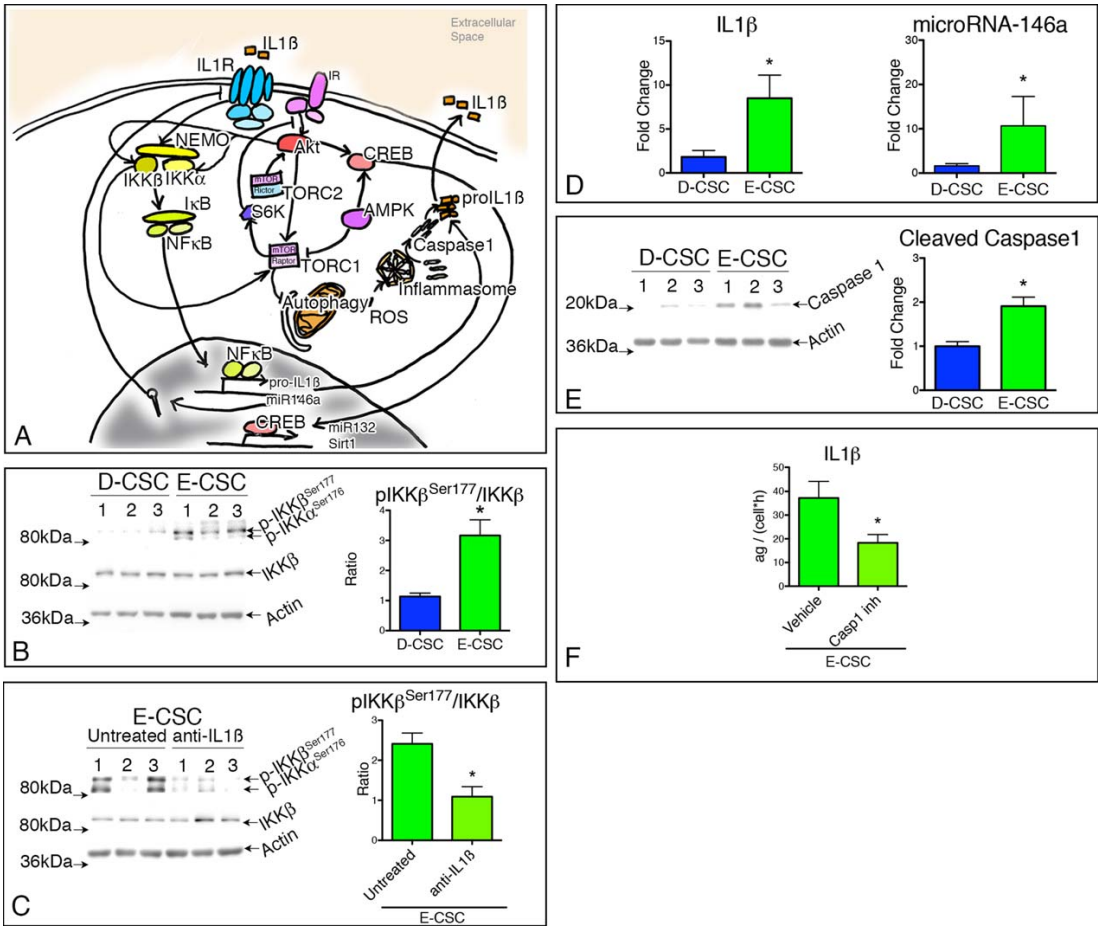

Figure 3. IL1β secretion is associated with an autocrine/paracrine loop that requires Caspase1 activity. Described interconnections between molecular pathways that have been associated both with paracrine (IL1β) and intrinsic cellular senescence are depicted in cartoon **(A)**. Sharp end arrows indicate activation, while blunt end arrows indicate repression. **(B, C, E)** Representative Western blots of cell extracts obtained from three D-CSC and three E-CSC (B, E), and three E-CSC either treated or not with an anti-IL1β antibody (C). Blotted proteins were incubated with antibodies directed against IKKβ, phospho-IKKβ^{Ser177} (B, C), and Caspase1 (E). Histograms (B, C, E) show the results of the densitometric analyses. Histograms in **(D)** show the expression levels of IL1β mRNA and microRNA-146a in D- and E-CSC. Histograms in **(F)** show the quantity of IL1β secreted by E-CSC either in the absence (Vehicle) or presence (Casp 1 inh) of the caspase 1 inhibitor Z-YVAD-FMK. *, $p < .05$ versus I bar. Abbreviations: CREB, cAMP response element-binding protein; D-CSC, cardiac stem cells isolated from donor hearts; E-CSC, cardiac stem cells isolated from explanted, failing hearts.

nM-, 10 nM-, 100 nM-, and 1 μM-rapamycin and 100 nM-, 0.5 μM-, 1 μM-, and 100 μM-resveratrol on CSC death, senescence, and proliferation (Supporting Information Fig. S5). Based on these results, we focused on dosages of rapamycin (10 nM) and resveratrol (0.5 μM) that reduce the fraction of senescent E-CSC and are below the threshold of cytotoxicity (Supporting Information Fig. S5). Both drugs reduce the frequency of p16-positive E-CSC with no supplemental effect with drug combination (Supporting Information Fig. S6Ai), while the latter was required to reduce DNA damage as assessed by measurement of γH2AX in Ki67-negative cells (Supporting Information Fig. S6Aii). Moreover, rapamycin induced a slight increase in the fraction of apoptotic E-CSC while resveratrol produced the opposite effect; hence, the two drugs nullified each other with regard to apoptosis, when tested in combination (Supporting Information Fig. S6Aiii). Cell migration was seemingly improved by resveratrol only (Supporting Information Fig. S6Av), with no additive effect by combined treatment. This latter significantly increased the fraction of cycling cells, although a significant increase in growth speed was induced only by resveratrol (Supporting Information Fig. S6Aiv, S6B). Intriguingly, drug treatment had a minimal effect on D-CSC, mainly increasing cell proliferation (data not shown).

Concerning molecular mechanisms, the combined drug treatment resulted in a significant increase in AMPK phosphorylation (Fig. 5A, 5B), a result that was not obtained treating CSC with the single drugs. When looking at other molecular nodes of the network, rapamycin was responsible for most of the observed effects. Specifically, it attenuated TORC1 signaling activation, as supported by the significant decrease in the phosphorylation of S6K on Thr^{389} (Fig. 5A,

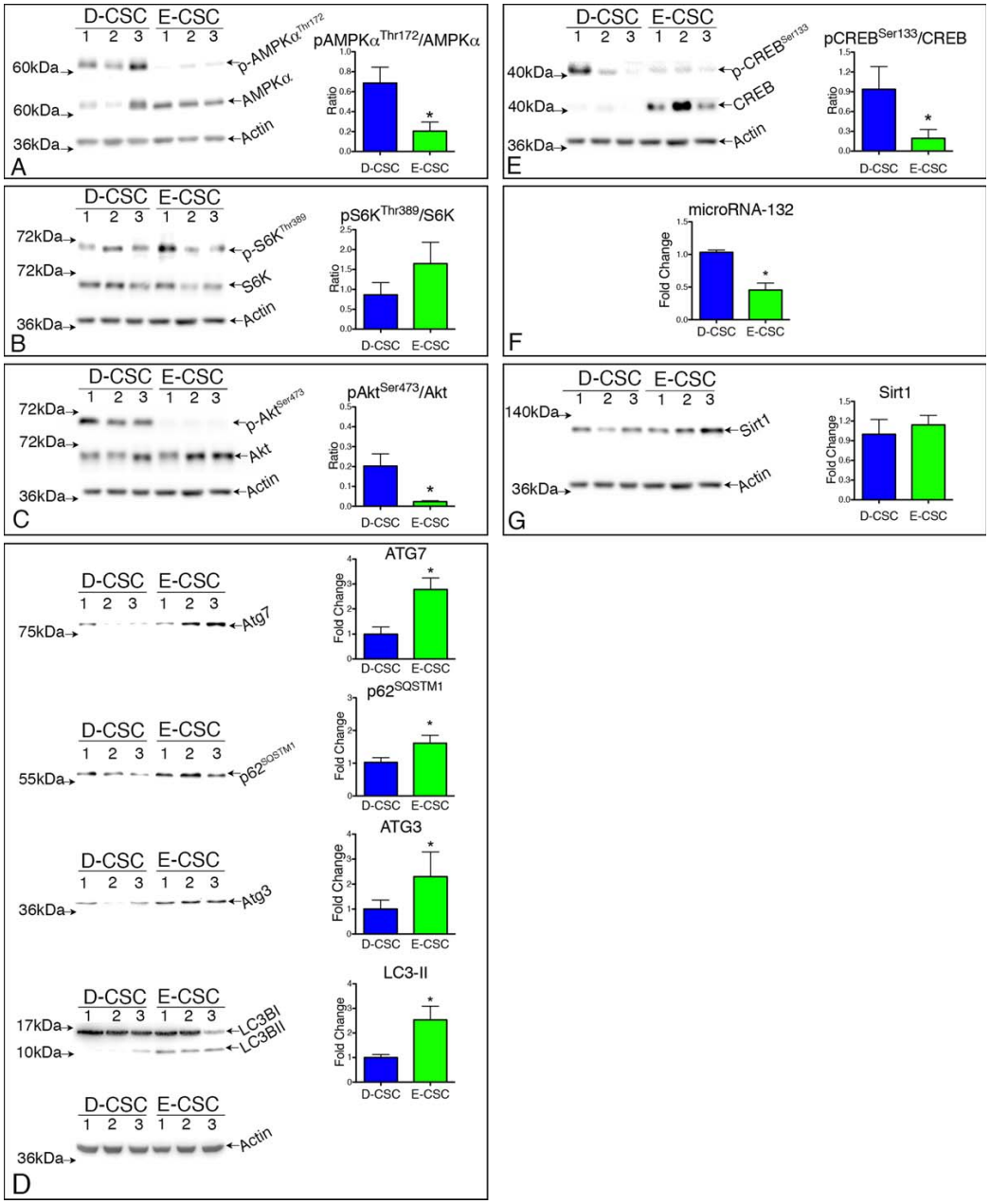

Figure 4. Senescent E-CSC show reduced AMPK, Akt, and CREB activating phosphorylation levels and increased TORC1 activity. **(A–D, E, G)**: Representative Western blots of cell extracts obtained from three D-CSC and three E-CSC. Blotted proteins were incubated with antibodies directed against AMPK, phospho-AMPKα^{Thr172} (A), S6K, phospho-S6K^{Thr389} (B), Akt, phospho-Akt^{Ser473} (C), Atg7, p62/SQSTM1, Atg3, and LC3B (D), CREB, phospho-CREB^{Ser133} (E), and Sirt1 (G). Histograms in (A–D, E, G) show the results of the densitometric analyses. Bar graphs in **(F)** show the expression of microRNA-132 in D- and E-CSC. *, $p < .05$ versus D-CSC. Abbreviations: CREB, cAMP response element-binding protein; D-CSC, cardiac stem cells isolated from donor hearts; E-CSC, cardiac stem cells isolated from explanted, failing hearts.

5C) and it significantly increased the phosphorylation of Akt on Ser^{473} (Fig. 5A, 5D). In addition, although none of these two drugs modified the expression of Beclin1, Atg3, Atg7, or LC3BII (Supporting Information Fig. S7), rapamycin significantly reduced p62/SQSTM1 levels (Fig. 5A, 5E), suggesting an improvement in the autophagic flux. Additionally, drug treatment, especially resveratrol, increased CREB phosphorylation on Ser^{133} (Fig. 5A, 5F) and its downstream targets Sirt1 (Fig. 5A, 5G) and microRNA-132 (Fig. 5A, 5H). Last, although drug treatment did not modify either IKKβ phosphorylation

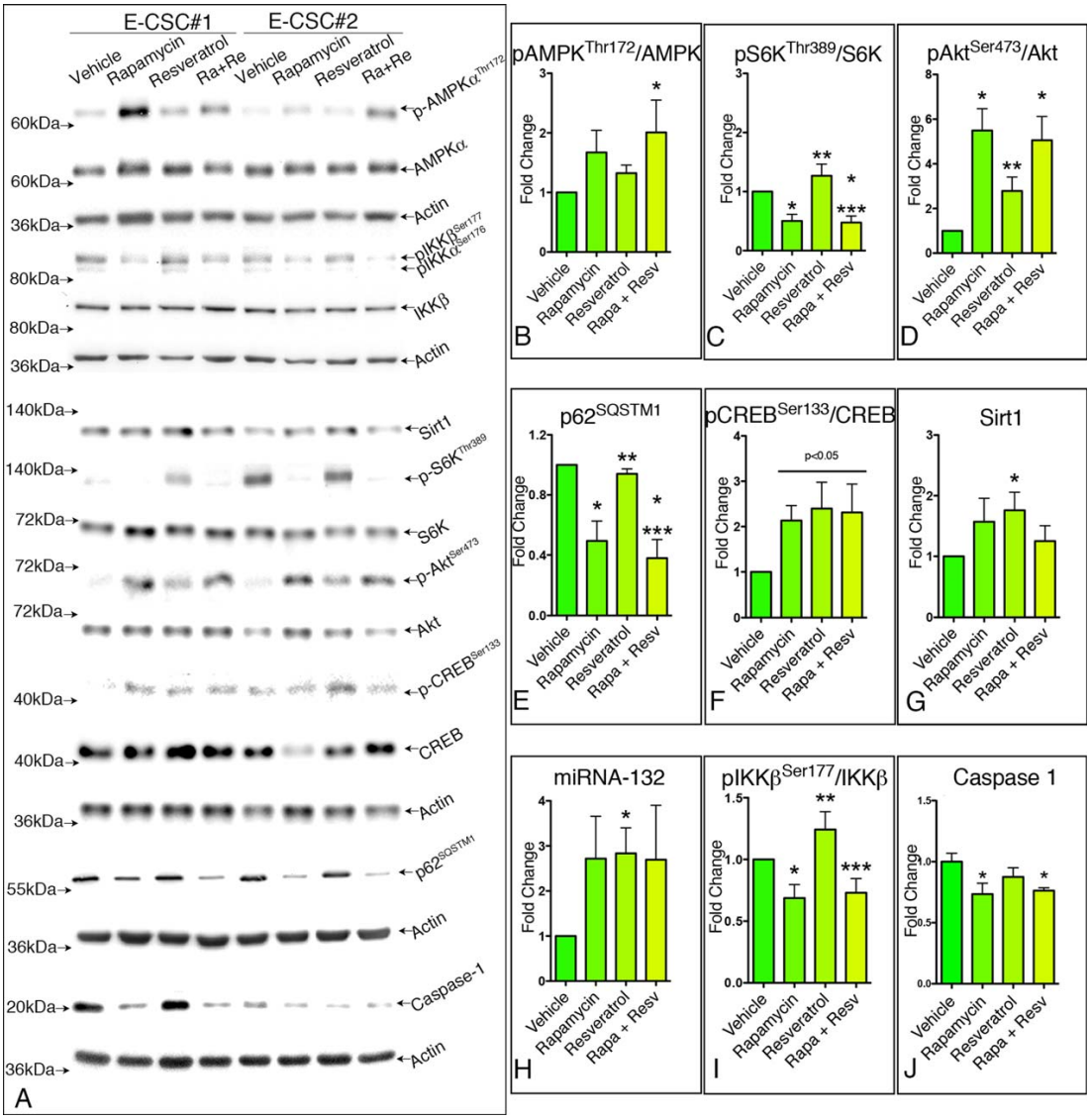

Figure 5. Effects of rapamycin and resveratrol treatment on E-CSC. Western blot of cell extracts obtained from two E-CSC (E-CSC #1, and E-CSC#2) showing the effect of drug treatment on AMPK, phospho-AMK^{Thr172}, S6K, phospho-S6K^{Thr389}, Akt, phospho-Akt^{Ser473}, p62/SQSTM1, CREB, phospho-CREB^{Ser133}, Sirt1, IKKβ, phospho-IKKβ^{Ser177}, and cleaved Caspase 1 levels **(A)**. Densitometric analysis of WB and relative expression of microRNA-132 are shown in histograms **(B–J)**. *, **, ***, $p < .05$ versus vehicle, rapamycin, and resveratrol, respectively. Abbreviations: CREB, cAMP response element-binding protein; E-CSC, cardiac stem cells isolated from explanted, failing hearts.

(Fig. 5A, 5I) or IL1β and microRNA-146a transcript levels (data not shown), it significantly reduced the levels of activated Caspase 1 (Fig. 5A, 5J). Importantly, preconditioning of E-CSC with resveratrol and rapamycin modified the secretory profile of these cells, remarkably decreasing the release of IL1β (Supporting Information Fig. S8A). As a consequence, drug treatment partly restored the ability of E-CSC secretome to protect cardiomyocytes exposed to SI/RO injury from senescence and apoptosis (Supporting Information Fig. S8B). In contrast, drug treatment had no effect on the biological activity of D-CSC secretome (Supporting Information Fig. S9).

Altogether these results indicate that a 3-day long pharmacologic treatment of E-CSC with a combination of rapamycin and resveratrol reduces the fraction of cells affected by cell senescence and increases their proliferative rate. These improvements are associated with increased AMPK phosphorylation. Most importantly, drug treatment reduced IL1β secretion and restored the protective effects of E-CSC secretome.

In Vitro Pharmacologic Pretreatment of Senescent CSC Improves Their In Vivo Reparative Potential

Last, we verified if CSC obtained from end-stage failing hearts favor myocardial repair as efficiently as those obtained from

normal hearts. Additionally, we investigated if rescuing the senescent traits of E-CSC ex vivo would translate into improved outcomes of cell therapy. To this aim, infarcted, immunodeficient mice ($n = 70$) were injected with either vehicle ($n = 17$ mice), CSC obtained from eight healthy human hearts ($n = 18$ mice), or CSC obtained from seven explanted human hearts ($n = 17$ mice). Additionally, five different E-CSC lines were exposed for 3 days to resveratrol and rapamycin and 2 days later implanted in the infarct border zone, in the same animal model ($n = 18$) described above.

Cell therapy with any of the three cell types improved cardiac output; however, D-CSC outperformed E-CSC with respect to both cardiac dimensional parameters, including left ventricle anterior wall thickness and left ventricle end systolic volume, and functional indexes, including left ventricle stroke volume, left ventricle ejection fraction, left ventricle fractional shortening, and dP/dt (Fig. 6A). Importantly, animals implanted with ex vivo conditioned E-CSC (TR-E-CSC) showed an improvement in cardiac dimensional and functional parameters compared with animals given nonconditioned media, thus matching the results obtained in animals implanted with D-CSC (Fig. 6A).

Moreover, we observed a reduction in scar size only if D-CSC or drug-treated E-CSC were used for cell therapy (Fig. 6B). These results were coupled with an angiogenic boost, where D-CSC increased the tissue density of capillaries and small arterioles, while TR-E-CSC incremented the density of larger arterioles (Fig. 6C). Treatment with D-CSC protected cardiomyocytes residing in the peri-infarct region (border-zone) from cell apoptosis (Fig. 7A, 7D) and senescence (Fig. 7B, 7I). E-CSC treatment not only lacked such a protective effect, but was also associated with an increase in myocyte apoptosis and senescence in the remote myocardium (Fig. 7D, 7I). Importantly, rapamycin and resveratrol partially restored the positive impact of this cell type. Similar effects were also observed on the frequency of cycling myocytes residing in the border-zone (Fig. 7C, 7E).

Cell therapy may favor myocardial repair by recruiting endogenous CSC to the site of myocardial damage [37]. Consistently, we observed a significant increase in the frequency of cardiac primitive/progenitor cells in D-CSC and TR-E-CSC injected animals, while E-CSC treatment failed in recruiting primitive cells (Fig. 7F–7H, 7J).

Altogether these data indicate that, although E-CSC show a blunted in vivo reparative ability, pharmacologic preconditioning with rapamycin and resveratrol restores the capacity of these cells to facilitate myocardial healing and to improve cardiac performance.

Discussion

Previously, we have shown that a large fraction of CSC isolated from failing hearts is affected by cell senescence processes [5]. In this study, we newly identify key molecular mechanisms of this accrued senescence. This could be traced back to an altered secretome, which is remarkably enriched with IL1β, a potent proinflammatory cytokine that plays a primary role in the pathophysiology of cardiovascular disease and heart failure [38]. Consistently, we provide evidence that IL1β weakens the protective effect of E-CSC on the apoptosis and senescence of adult cardiomyocytes exposed to SI/RO in vitro. In fact, the secretome released by senescent cells (SASP) plays a crucial role in aging and age-related pathologies, since it may reinforce senescence autocrinally or induce senescence paracrinally [39]. Importantly, recent data have demonstrated that the entire SASP process is orchestrated by IL1 secretion that follows inflammasome activation [10]. This latter is a crucial event that may be triggered by danger signals (e.g., ATP, high-mobility group protein B1, free fatty acids, islet amyloid polypeptide, and mono-sodium uric acid crystals) or by reactive oxygen species (ROS) [40]. Importantly, the accumulation of these latter has been associated, in myeloid cells, with an impairment of the autophagic flux that follows a decrease in AMPK activity [12]. Therefore, we decided to compare the status of this pathway in D- and E-CSC.

Noteworthy, we found that AMPK is less phosphorylated in E-CSC than in control D-CSC, in analogy to what observed both in cardiomyocytes isolated from spontaneously hypertensive rats or in cardiac tissue of doxorubicin-treated rats [41, 42]. Given the central role played by AMPK in regulating cell metabolism, this result is corroborated by our previous gene expression findings [5], which showed a different expression of gene sets associated with lipid-, carbohydrate-, and amino acid-metabolism between D- and E-CSC. We further demonstrate that the activation status of several molecular pathways interconnected with AMPK signaling is significantly perturbed in E-CSC. Among the most prominent ones, we show that E-CSC have an enhanced TORC1 activity, as supported by a trend toward increased phospho-S6K^{Thr389} levels, a block in the autophagic flux (i.e., an accumulation of autophagic markers in the absence of reduced p62/SQSTM1 levels) and a reduction in Akt activation [18]. Although several lines of evidence indicate that mTOR plays a prominent role in cellular senescence and organismal aging [43], the exact mechanism leading to the activation of TORC1 is less clear. Our results indicate that, in senescent E-CSC, AMPK may cooperate with autocrine/paracrine inflammatory signals to activate mTOR in a PI3K/Akt-independent fashion. These data are consistent with the proven ability of IL1β to stimulate TORC1 activity via IKKβ [15].

In addition, the reduced activation of Akt, observed in E-CSC, may be responsible, at least in part, for the decreased activating phosphorylation of CREB on Ser^{133} that attenuates this signaling pathway in E-CSC [36]. Our observations are consistent with the impaired CREB signaling characterizing senescent fibroblasts [44]. In senescent cells, a defective activation of CREB pathway is reportedly coupled with the altered circadian expression of clock genes, possibly via a mechanism that involves microRNA-132 [24, 44, 45].

Moving from these observations, we decided to use: (a) rapamycin, a TORC1 inhibitor, that may also activate AMPK [46], and (b) resveratrol for its ability to activate AMPK and possibly CREB, elevating intracellular cAMP levels [47]. We demonstrate here for the first time that rapamycin and resveratrol cooperate to activate AMPK. Rapamycin acted mostly inhibiting S6K^{Thr389} phosphorylation, increasing Akt^{Ser473} phosphorylation, and reversing the autophagic arrest, thus suggesting that TORC1 was required for these events [18]. Resveratrol given at a very low dose (0.5 μM) acted

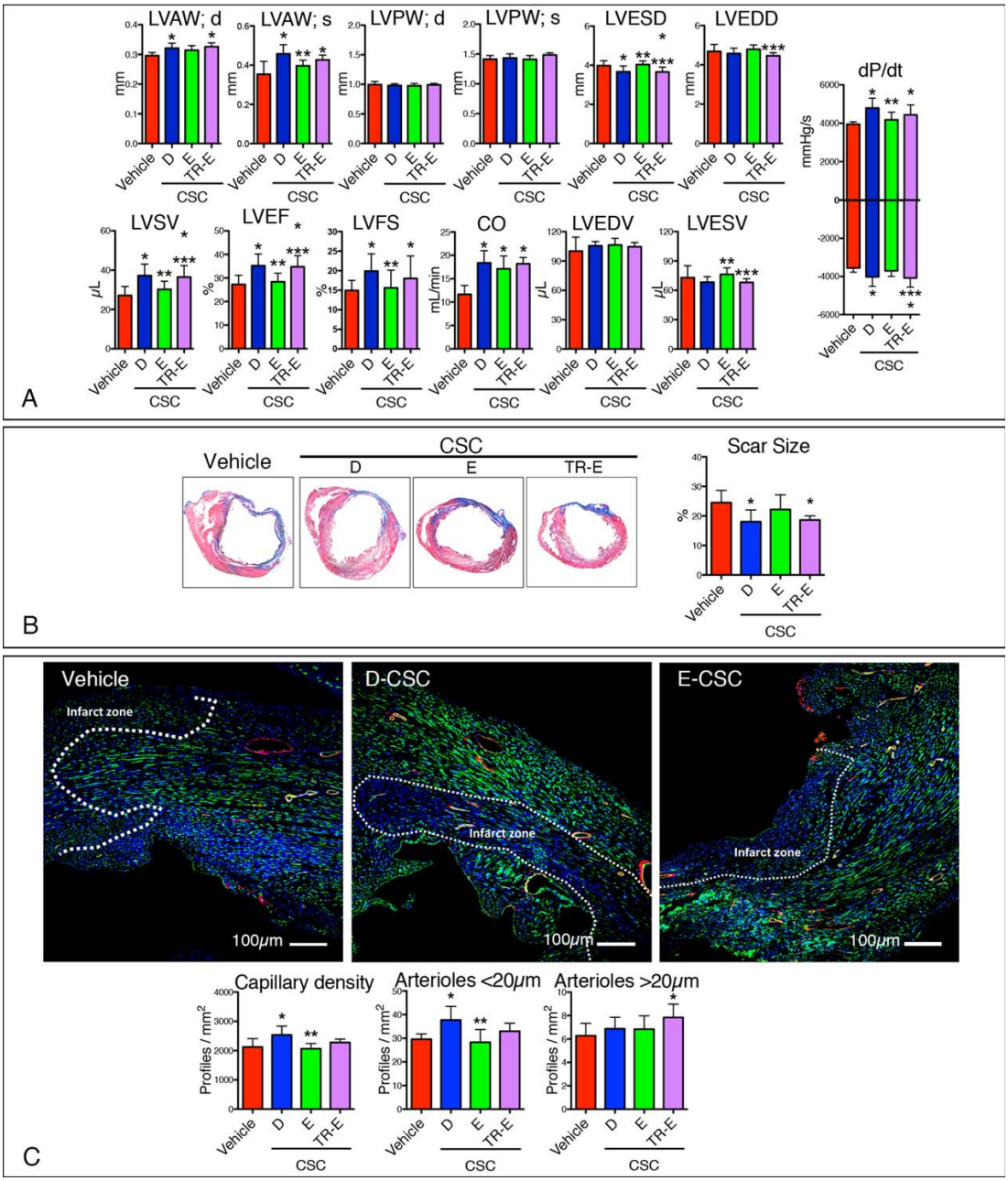

Figure 6. Pretreatment of E-CSC with rapamycin and resveratrol restores their ability to repair infarcted murine hearts. Bar graphs showing anatomic and hemodynamic parameters **(A)** of infarcted mouse hearts injected either with Vehicle ($n = 17$), D-CSC ($n = 18$), E-CSC ($n = 17$), or drug treated (TR) E-CSC ($n = 18$) 14 days post-MI. Trichrome staining of transverse sections of infarcted mouse hearts injected with Vehicle, D-CSC, E-CSC, or TR-E-CSC **(B)**. Bar graphs show the volume fraction of myocardium occupied by the scar. Epifluorescence images of Isolectin B4 (green), α-smooth muscle actin (red), and nuclear (blue) staining of infarcted mouse hearts injected with either Vehicle, D-CSC, or E-CSC (C, upper panels). Bar graphs in the lower panels show the measured density of capillaries, small (< 20 μm in diameter) and large (> 20 μm in diameter) arterioles. Values are means ± SEM. *, **, ***, $p < .05$ versus Vehicle, D-CSC, and E-CSC, respectively. Abbreviations: CO, cardiac output; D-CSC, cardiac stem cells isolated from donor hearts; d, diastole; E-CSC, cardiac stem cells isolated from explanted, failing hearts; LVAW, left ventricle anterior wall thickness; LVPW, left ventricle posterior wall thickness; LVESD, left ventricle end systolic diameter; LVEDD, left ventricle end diastolic diameter; LVESV, left ventricle end systolic volume; LVEDV, left ventricle end diastolic volume; LVSV, left ventricle stroke volume; LVEF, left ventricle ejection fraction; LVFS, left ventricle fractional shortening; s, systole.

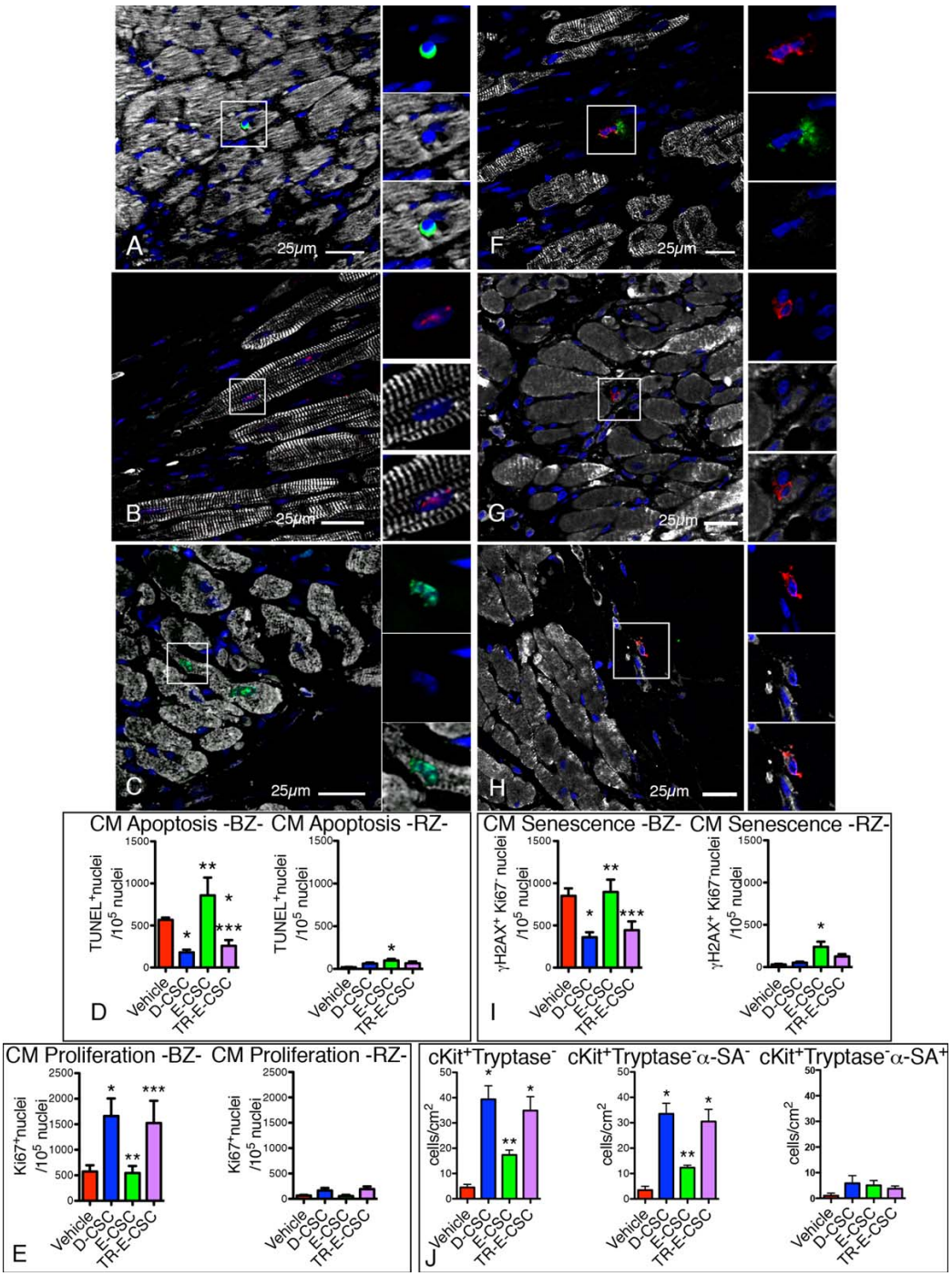

Figure 7. Rapamycin and resveratrol restore the ability of E-CSC to repair infarcted murine hearts. Confocal images of TUNEL positive (green nuclear positivity) apoptotic cardiomyocytes **(A)**, senescent myocytes (γH2AX red nuclear positivity in Ki67-negative cells) **(B)**, and cycling cardiomyocytes (Ki67 nuclear positivity, green) **(C)**. Myocyte cytoplasm is labeled by α-sarcomeric actin (α-SA, white), while 4′,6-diamidino-2-phenylindole labels nuclei in blue. Histograms **(D, E, I)** summarize quantitative data. Confocal images of a representative mastocyte (cKit$^+$/mast-cell tryptase$^+$ cell, **F**), cardiac stem/progenitor cell (cKit$^+$/α-SA$^-$ cell, **G**), and myocyte precursor (cKit$^+$/α-SA$^+$ cell, **H**). cKit is depicted in red, tryptase in green, α-SA in white, nuclei in blue. Histograms summarizing quantitative data on the density of total cKit$^+$/Tryptase$^-$ cells, stem/progenitor cells, and precursors in the left ventricle **(J)**. *, **, ***, $p < .05$ versus Vehicle, D-CSC, and E-CSC, respectively. Abbreviations: D-CSC, cardiac stem cells isolated from donor hearts; E-CSC, cardiac stem cells isolated from explanted, failing hearts.

mainly potentiating CREB phosphorylation which, in turn, incremented microRNA-132 and Sirt1 expression. However, drug treatment did not modify IKKβ phosphorylation or NF-κB signaling. This result is consistent with the observed activation of Akt upon exposure to rapamycin and resveratrol, since a complex crosstalk between these two pathways is well established [48].

Importantly, we demonstrated that rapamycin and resveratrol reduce by approximately 80% IL1β secretion, thus restoring the ability of E-CSC secretome to prevent cardiomyocyte death and senescence. Since NF-κB signaling was not significantly modified by drug treatment, our data suggest that rapamycin and resveratrol act reducing the activation of Caspase 1. In line with our findings, recent pilot clinical trials have started to experiment the use of IL1β blockade (with Anakira, a recombinant human IL1Ra) both in acute MI [49, 50] and chronic heart failure [51]. In this latter group, Anakira reduced the levels of plasmatic IL1 by nearly 90%, supporting the notion that IL1 follows a positive feedback loop in heart failure [38].

Last, we newly demonstrated that microRNA-132, a critical mediator of the beneficial effects of cell therapy that was recently described by our groups [32], although constitutively expressed by CSC, is reduced in senescent cells. Importantly, drug treatment reversed this alteration.

Although cellular senescence is strongly associated with age-related pathologies [3, 4], this cellular process plays an uncertain role in tissue repair in vivo, since it could be transiently required for proper healing of injuries by releasing paracrine factors [52]. This hypothesis has never been tested in acute MI. This work newly documents that senescent CSC repair cardiac injury in vivo less effectively than nonsenescent ones. The implantation of senescent CSC in the border zone of infarcted murine hearts does not enhance either angiogenesis or cardiomyocyte proliferation, while it increases myocyte senescence and apoptosis, suggesting that E-CSC may exert a negative paracrine effect. These results are in line with recent data obtained by Naftali-Shani et al., who showed the proinflammatory properties of human cardiac mesenchymal stem cells obtained from failing hearts [53]. Strikingly, the same, IL1-based, mechanism for stem cell dysfunction was shown to impair the ability of bone marrow cells, obtained from donor infarcted mice, to repair MI in syngeneic animals [54].

Finally, we demonstrated that the ex vivo pretreatment of E-CSC with rapamycin and resveratrol was able to restore their reparative potential to levels observed with D-CSC. This effect consisted of an enhanced arteriolar density, decreased cardiomyocyte senescence and apoptosis, and increased recruitment of host CSC, which were anatomically mirrored by reduced infarct size and functionally corresponded by improvement of contractility indexes. However, our animal study has been possibly limited by the lack of post-MI echocardiographic baseline data and the short (2 weeks) follow-up.

The wide range of effects exerted by ex vivo preconditioning suggests that rejuvenated E-CSC act through direct and indirect means probably via paracrine influence on various cellular components of the infarcted heart [55]. These results indicate for the first time that the moderate effect of cell therapy using senescent CSC can be strikingly enhanced by ex vivo preconditioning with antiaging drugs. The therapeutic effect of drug-rejuvenated CSC is twofold relevant: it invigorates the use of autologous cell treatment (as results were superimposable with that of D-CSC) and represents a less risky approach with respect of genetic modification strategies.

Recently, a work by Cheng et al. has suggested that cardiosphere-derived cells (CDC) obtained from advanced heart failure patients exhibit higher reparative potential than CDC obtained from donated hearts [56]. The observed discrepancy between our results and this work may be related to a series of technical differences. Specifically, Cheng obtained CDC from the septum, while we obtained CSC from atrial tissue, the richest source of CSC [57]. Additionally, as normal control, we grew D-CSC from discarded atrial fragments of donated hearts collected at time of transplantation, while Cheng expanded Normal-CDC from endomyocardial biopsies of donated hearts after their implantation in recipient, failing patients under immunosuppressive regimens.

Conclusions

Our data indicate that senescent CSC obtained from end-stage failing hearts show an impaired reparative ability in vivo. AMPK, Akt/mTOR/S6K, and CREB pathways play a central role in this process. Importantly, the pathologic phenotype is not irreversible. The translational relevance of our work is supported by the fact that recently autologous CSC-based clinical trials showed preliminary evidence of therapeutic efficacy [6, 7]. Based on this work, we provide evidence that E-CSC-based cell therapy may be suboptimal. Moreover, we demonstrate that a very short pharmacologic conditioning could rejuvenate, without the requirement for the genetic manipulation of cells [58], patient-derived cells, boosting in vivo cardiac regeneration. This finding opens new avenues for optimal regenerative treatments with autologous CSC.

Acknowledgments

This work was supported by Italian Ministry of Health, G.R.-2007-683407 (D.C.), Project ERC-7FP SP 2 IDEAS QUIDPROQUO G.A. n. 269051, Title: "Molecular nanotechnology for life science applications: quantitative interactomics for diagnostics, proteomics and quantitative oncology" (G.S., D.C. and A.P.B.), human pericyte progenitor cells and cardiac progenitor cells for specialized stimulation of neovascularisation and cardiomyogenesis of the infarcted heart, BHF Project Grant (P.M.), and National Health Research Institute, BRU grant (P.M.).

Author Contributions

E. Avolio, G.G., and A.C.: planned experiments, performed experiments, and analyzed data; D.C.: planned experiments, performed experiments, analyzed data, and wrote the article; E. Athanasakis, R.K., M.M., A.P., A.B., C.V., B.T., and E.M.: performed experiments and analyzed data; N.F., G.A., and U.L.: recruited patients and collected samples; C.E. and G.S.: critically evaluated article draft; C.A.B.: wrote article, and critically evaluated article draft; P.M.: planned experiments,

wrote article, and critically evaluated article draft; A.P.B.: planned experiments, analyzed data, and wrote article. E.A. and G.G. contributed equally to this article.

Disclosure of Potential Conflicts of Interest

The authors indicate no potential conflicts of interest.

References

1 Lawless C, Wang C, Jurk D, et al. Quantitative assessment of markers for cell senescence. Exp Gerontol 2010;45:772–778.
2 Baker DJ, Sedivy JM. Probing the depths of cellular senescence. J Cell Biol 2013;202:11–13.
3 Beltrami AP, Cesselli D, Beltrami CA. At the stem of youth and health. Pharmacol Ther 2011;129:3–20.
4 Beltrami AP, Cesselli D, Beltrami CA. Stem cell senescence and regenerative paradigms. Clin Pharmacol Ther 2012;91:21–29.
5 Cesselli D, Beltrami AP, D'Aurizio F, et al. Effects of age and heart failure on human cardiac stem cell function. Am J Pathol 2011;179:349–366.
6 Bolli R, Chugh AR, D'Amario D, et al. Cardiac stem cells in patients with ischaemic cardiomyopathy (SCIPIO): Initial results of a randomised phase 1 trial. Lancet 2011;378:1847–1857.
7 Makkar RR, Smith RR, Cheng K, et al. Intracoronary cardiosphere-derived cells for heart regeneration after myocardial infarction (CADUCEUS): A prospective, randomised phase 1 trial. Lancet 2012;379:895–904.
8 Cottage CT, Bailey B, Fischer KM, et al. Cardiac progenitor cell cycling stimulated by pim-1 kinase. Circ Res 2010;106:891–901.
9 Katare R, Oikawa A, Cesselli D, et al. Boosting the pentose phosphate pathway restores cardiac progenitor cell availability in diabetes. Cardiovasc Res 2013;97:55–65.
10 Acosta JC, Banito A, Wuestefeld T, et al. A complex secretory program orchestrated by the inflammasome controls paracrine senescence. Nat Cell Biol 2013;15:978–990.
11 Pope RM, Tschopp J. The role of interleukin-1 and the inflammasome in gout: Implications for therapy. Arthritis Rheum 2007;56:3183–3188.
12 Wen H, Gris D, Lei Y, et al. Fatty acid-induced NLRP3-ASC inflammasome activation interferes with insulin signaling. Nat Immunol 2011;12:408–415.
13 Salminen A, Kaarniranta K. AMP-activated protein kinase (AMPK) controls the aging process via an integrated signaling network. Ageing Res Rev 2012;11:230–241.
14 Laplante M, Sabatini DM. mTOR signaling in growth control and disease. Cell 2012;149:274–293.
15 Lee DF, Kuo HP, Chen CT, et al. IKK beta suppression of TSC1 links inflammation and tumor angiogenesis via the mTOR pathway. Cell 2007;130:440–455.
16 Korotchkina LG, Leontieva OV, Bukreeva EI, et al. The choice between p53-induced senescence and quiescence is determined in part by the mTOR pathway. Aging (Albany NY) 2010;2:344–352.
17 Gan B, DePinho RA. mTORC1 signaling governs hematopoietic stem cell quiescence. Cell Cycle 2009;8:1003–1006.
18 Huang J, Manning BD. A complex interplay between Akt, TSC2 and the two mTOR complexes. Biochem Soc Trans 2009;37(Pt 1):217–222.
19 Zoncu R, Efeyan A, Sabatini DM. mTOR: From growth signal integration to cancer, diabetes and ageing. Nat Rev Mol Cell Biol 2011;12:21–35.
20 Thomson DM, Herway ST, Fillmore N, et al. AMP-activated protein kinase phosphorylates transcription factors of the CREB family. J Appl Physiol (1985) 2008;104:429–438.
21 Hansen RT, 3rd, Zhang HT. Senescent-induced dysregulation of cAMP/CREB signaling and correlations with cognitive decline. Brain Res 2013;1516:93–109.
22 Fusco S, Ripoli C, Podda MV, et al. A role for neuronal cAMP responsive-element binding (CREB)−1 in brain responses to calorie restriction. Proc Natl Acad Sci USA 2012;109:621–626.
23 Noriega LG, Feige JN, Canto C, et al. CREB and ChREBP oppositely regulate SIRT1 expression in response to energy availability. EMBO Rep 2011;12:1069–1076.
24 Alvarez-Saavedra M, Antoun G, Yanagiya A, et al. miRNA-132 orchestrates chromatin remodeling and translational control of the circadian clock. Hum Mol Genet 2011;20:731–751.
25 Blagosklonny MV. Cell cycle arrest is not yet senescence, which is not just cell cycle arrest: Terminology for TOR-driven aging. Aging (Albany NY) 2012;4:159–165.
26 Li H, Xia N, Forstermann U. Cardiovascular effects and molecular targets of resveratrol. Nitric Oxide 2012;26:102–110.
27 Demidenko ZN, Blagosklonny MV. At concentrations that inhibit mTOR, resveratrol suppresses cellular senescence. Cell Cycle 2009;8:1901–1904.
28 Xia L, Wang XX, Hu XS, et al. Resveratrol reduces endothelial progenitor cells senescence through augmentation of telomerase activity by Akt-dependent mechanisms. Br J Pharmacol 2008;155:387–394.
29 Penumathsa SV, Thirunavukkarasu M, Zhan L, et al. Resveratrol enhances GLUT-4 translocation to the caveolar lipid raft fractions through AMPK/Akt/eNOS signalling pathway in diabetic myocardium. J Cell Mol Med 2008;12:2350–2361.
30 Dasgupta B, Milbrandt J. Resveratrol stimulates AMP kinase activity in neurons. Proc Natl Acad Sci USA 2007;104:7217–7222.
31 Cesselli D, D'Aurizio F, Marcon P, et al. Cardiac stem cell senescence. Methods Mol Biol 2013;976:81–97.
32 Katare R, Riu F, Mitchell K, et al. Transplantation of human pericyte progenitor cells improves the repair of infarcted heart through activation of an angiogenic program involving micro-RNA-132. Circ Res 2011;109:894–906.
33 Scheidereit C. IkappaB kinase complexes: Gateways to NF-kappaB activation and transcription. Oncogene 2006;25:6685–6705.
34 McMillan DH, Woeller CF, Thatcher TH, et al. Attenuation of inflammatory mediator production by the NF-kappaB member RelB is mediated by microRNA-146a in lung fibroblasts. Am J Physiol Lung Cell Mol Physiol 2013;304:L774–781.
35 Halkein J, Tabruyn SP, Ricke-Hoch M, et al. MicroRNA-146a is a therapeutic target and biomarker for peripartum cardiomyopathy. J Clin Invest 2013;123:2143–2154.
36 Du K, Montminy M. CREB is a regulatory target for the protein kinase Akt/PKB. J Biol Chem 1998;273:32377–32379.
37 Hatzistergos KE, Quevedo H, Oskouei BN, et al. Bone marrow mesenchymal stem cells stimulate cardiac stem cell proliferation and differentiation. Circ Res 2010;107:913–922.
38 Van Tassell BW, Toldo S, Mezzaroma E, et al. Targeting interleukin-1 in heart disease. Circulation 2013;128:1910–1923.
39 Coppe JP, Desprez PY, Krtolica A, et al. The senescence-associated secretory phenotype: The dark side of tumor suppression. Annu Rev Pathol 2010;5:99–118.
40 Lee HM, Kim JJ, Kim HJ, et al. Upregulated NLRP3 inflammasome activation in patients with type 2 diabetes. Diabetes 2013;62:194–204.
41 Gratia S, Kay L, Potenza L, et al. Inhibition of AMPK signalling by doxorubicin: At the crossroads of the cardiac responses to energetic, oxidative, and genotoxic stress. Cardiovasc Res 2012;95:290–299.
42 Dolinsky VW, Chan AY, Robillard Frayne I, et al. Resveratrol prevents the prohypertrophic effects of oxidative stress on LKB1. Circulation 2009;119:1643–1652.
43 Johnson SC, Rabinovitch PS, Kaeberlein M. mTOR is a key modulator of ageing and age-related disease. Nature 2013;493:338–345.
44 Chin JH, Okazaki M, Frazier JS, et al. Impaired cAMP-mediated gene expression and decreased cAMP response element binding protein in senescent cells. Am J Physiol 1996;271(1 Pt 1):C362–371.
45 Kunieda T, Minamino T, Katsuno T, et al. Cellular senescence impairs circadian expression of clock genes in vitro and in vivo. Circ Res 2006;98:532–539.
46 Habib SL. Mechanism of activation of AMPK and upregulation of OGG1 by rapamycin in cancer cells. Oncotarget 2011;2:958–959.
47 Park SJ, Ahmad F, Philp A, et al. Resveratrol ameliorates aging-related metabolic phenotypes by inhibiting cAMP phosphodiesterases. Cell 2012;148:421–433.
48 Vaughan S, Jat PS. Deciphering the role of nuclear factor-kappaB in cellular senescence. Aging (Albany NY) 2011;3:913–919.
49 Abbate A, Kontos MC, Grizzard JD, et al. Interleukin-1 blockade with anakinra to prevent adverse cardiac remodeling after acute myocardial infarction (Virginia Commonwealth University Anakinra Remodeling Trial [VCU-ART] Pilot study). Am J Cardiol 2010;105:1371–1377 e1.
50 Abbate A, Van Tassell BW, Biondi-Zoccai G, et al. Effects of interleukin-1 blockade

with anakinra on adverse cardiac remodeling and heart failure after acute myocardial infarction [from the Virginia Commonwealth University-Anakinra Remodeling Trial (2) (VCU-ART2) pilot study]. Am J Cardiol 2013; 111:1394–1400.

51 Van Tassell BW, Arena RA, Toldo S, et al. Enhanced interleukin-1 activity contributes to exercise intolerance in patients with systolic heart failure. PLoS One 2012;7: e33438.

52 Rodier F, Campisi J. Four faces of cellular senescence. J Cell Biol 2011;192:547–556.

53 Naftali-Shani N, Itzhaki-Alfia A, Landa-Rouben N, et al. The origin of human mesenchymal stromal cells dictates their reparative properties. J Am Heart Assoc 2013;2: e000253.

54 Wang X, Takagawa J, Lam VC, et al. Donor myocardial infarction impairs the therapeutic potential of bone marrow cells by an interleukin-1-mediated inflammatory response. Sci Transl Med 2011;3:100ra90.

55 Barile L, Lionetti V. Prometheus's heart: What lies beneath. J Cell Mol Med 2012;16: 228–236.

56 Cheng K, Malliaras K, Smith RR, et al. Human cardiosphere-derived cells from advanced heart failure patients exhibit augmented functional potency in myocardial repair. JACC Heart Fail 2014;2:49–61.

57 Itzhaki-Alfia A, Leor J, Raanani E, et al. Patient characteristics and cell source determine the number of isolated human cardiac progenitor cells. Circulation 2009;120:2559–2566.

58 Mohsin S, Khan M, Nguyen J, et al. Rejuvenation of human cardiac progenitor cells with Pim-1 kinase. Circ Res 2013;113: 1169–1179.

See www.StemCells.com for supporting information available online.